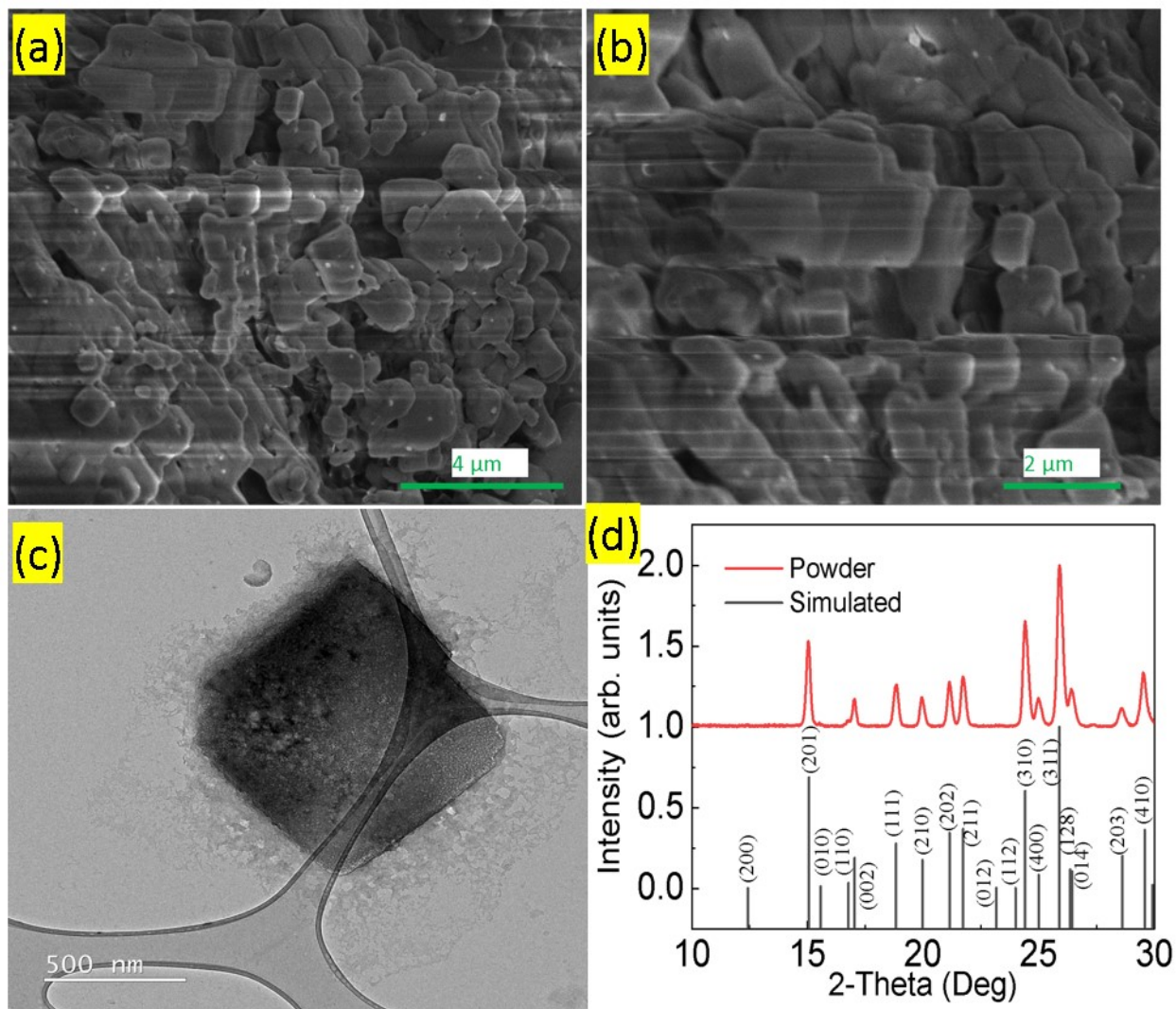


*Supplementary Information*

**Spherulite-enhanced Macroscopic Polarization in Molecular  
Ferroelectric Films from Vacuum Deposition**

## Supplementary Note 1. Characterizations for powder DC-MBI

5,6-Dichloro-2-methylbenzimidazole (DC-MBI) was brought from TCI, US. The powder sample morphologies were observed through Scanning Electron Microscope (**Fig. S1a** & **Fig. S1b**) and through Transmission electron microscope (**Fig. S1c**). The sample was further examined through X-ray diffraction (**Fig. S1d**) and compared to database (CCDC 909439).



**Figure S1.** **Fig (a &b)** are SEM (3 kV) images at different resolutions while **Fig(c)** is TEM (200 keV) images for powder DC-MBI and **Fig(d)** is the XRD for simulated and powder sample.

## Supplementary Note 2. Characterizations for DC-MBI films

DC-MBI films were deposited at substrate temperature  $T_s = 183$  K on various substrates. **Fig. S2** shows the closeup view of spherulite and dendrites and the corresponding Scanning Electron Microscope. SEM images clearly show the microscopic arrangements of the fibers as observed on the as grown films. The morphological distributions were similar on various substrates: **Fig. S3a and Fig. S3b** shows the cross-polarized images on gold plated Silicon substrate and IDE substrate respectively. **Fig. S4** shows qualitative comparison for the powder and films of DC-MBI as observed through X-ray Photoemission Spectroscopy (XPS). **Table 1** shows the statistics of the various types of morphologies as observed on the films grown on sapphire substrate. **Fig. S5** shows the detrimental effect on film morphologies on annealing at higher temperature suggesting for lower (353 K) annealing temperature to preserve the film morphologies and improve crystallinity.

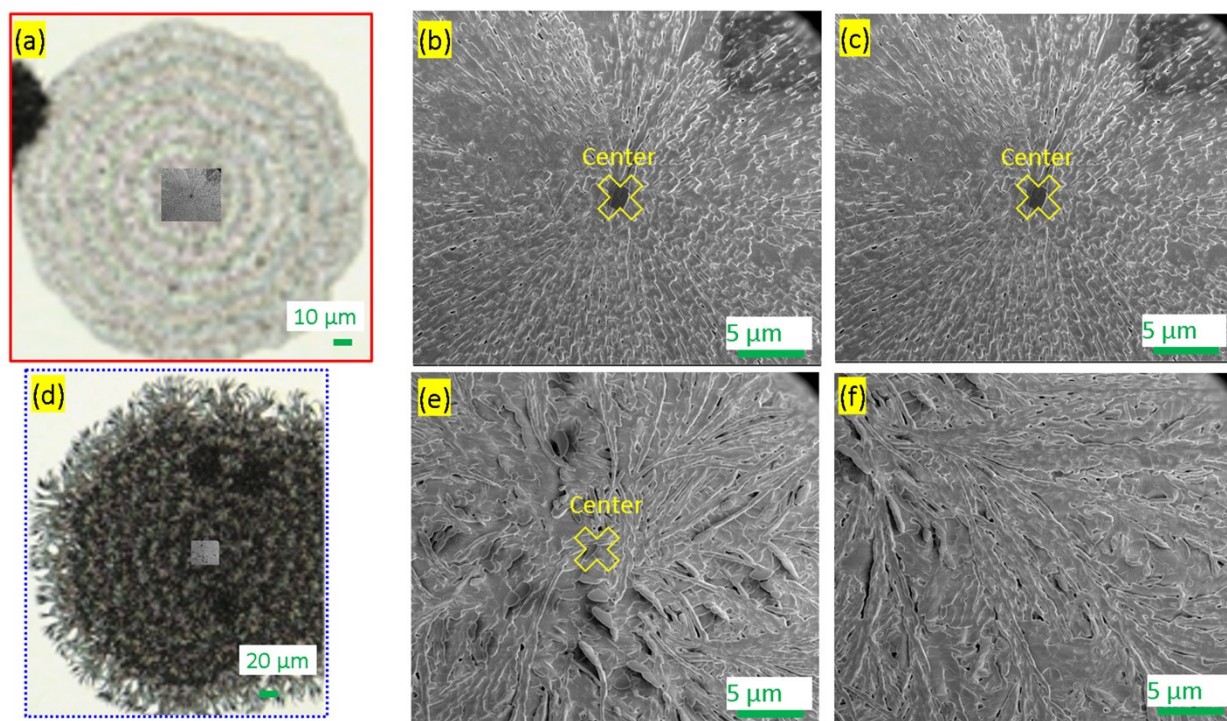


**Figure S2.** Fig (a & b) are the closeup view of Type-I and Type-II features as observed on laser microscope. Fig (b & c) are SEM images for Type-I while Fig (e & f) are corresponding SEM images for Type-II feature.

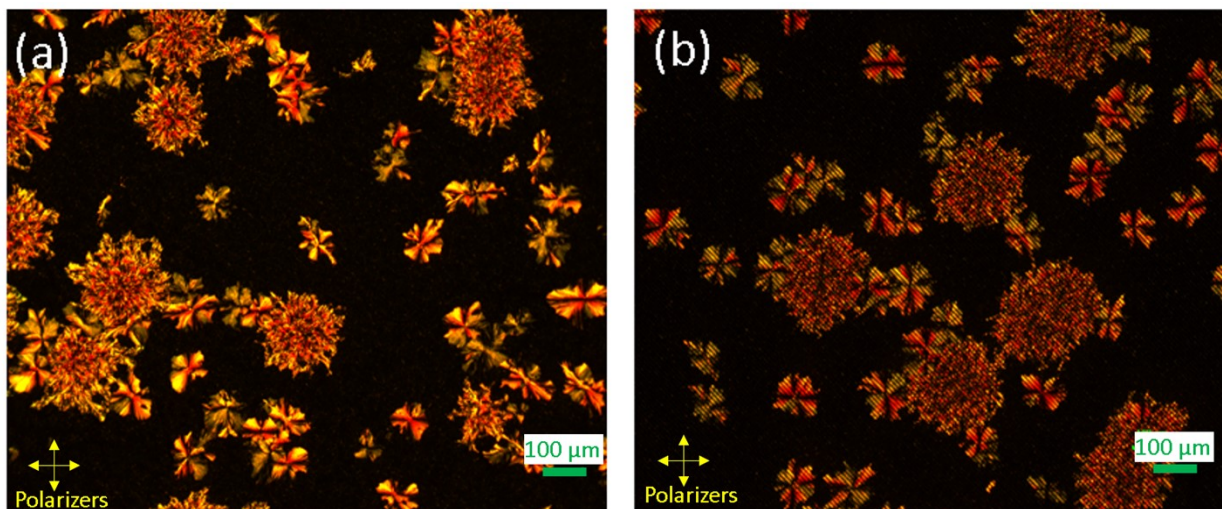


**Figure S3.** Crossed Polarized Images for the 2  $\mu\text{m}$  DC-MBI films grown on gold plated silicon substrate (a) and Pt Interdigitated Electrodes (b).

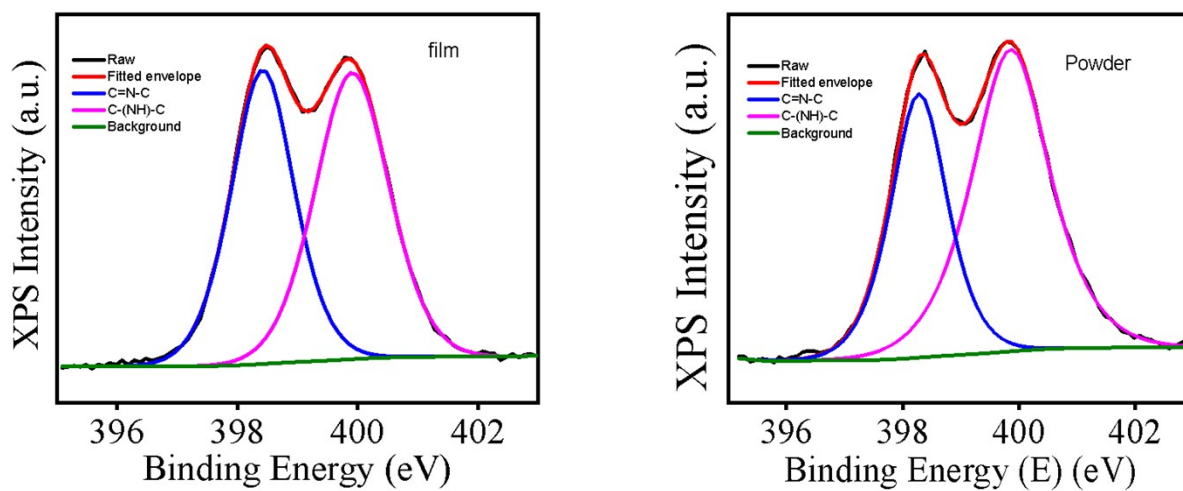


**Figure S4.** XPS data for Nitrogen Scan with peak fitting<sup>1</sup>. The figure on the left is for the film while that on right is for powder. Sample thickness is 4  $\mu\text{m}$ .

**Table S1.** Statistics (Average height and rms roughness) of features observed on sapphire substrate for DC-MBI grown at different substrate temperatures.

Temperature (K)	Spherulite: Type-I ( $H_{\text{avg}} \pm R_q$ ) ( $\mu\text{m}$ )	Dendrite: Type-II ( $H_{\text{avg}} \pm R_q$ ) ( $\mu\text{m}$ )	Black, small patches ( $H_{\text{avg}} \pm R_q$ ) ( $\mu\text{m}$ )
294	1 $\pm$ 0.70		7 $\pm$ 5.7
273	1 $\pm$ 0.6	2 $\pm$ 1.2	4 $\pm$ 1.7
223	0.5 $\pm$ 0.5	2 $\pm$ 1.3	8 $\pm$ 4
198	1.5 $\pm$ 1.0	8 $\pm$ 4	3.8 $\pm$ 2.1
183	1.4 $\pm$ 0.85	4.5 $\pm$ 3.4	3.7 $\pm$ 1.2
173	1.4 $\pm$ 0.6	2.5 $\pm$ 1.5	3 $\pm$ 2.5
163		3.5 $\pm$ 1.5	3 $\pm$ 1.0

### Supplementary Note 3. Electrical measurements for DC-MBI films

The DC-MBI films were deposited at  $T_s = 183$  K on IDE substrates and the corresponding electric displacement (D) and the voltage (V) graph measured for various thickness (**Fig. S5**) show the linear behavior. The local PFM measurements were conducted on the DC-MBI films deposited over the gold substrate to qualitatively demonstrate the microscopic switchable polarization. **Fig. S6** and **Fig. S7** show corresponding PFM and poling measurements respectively.

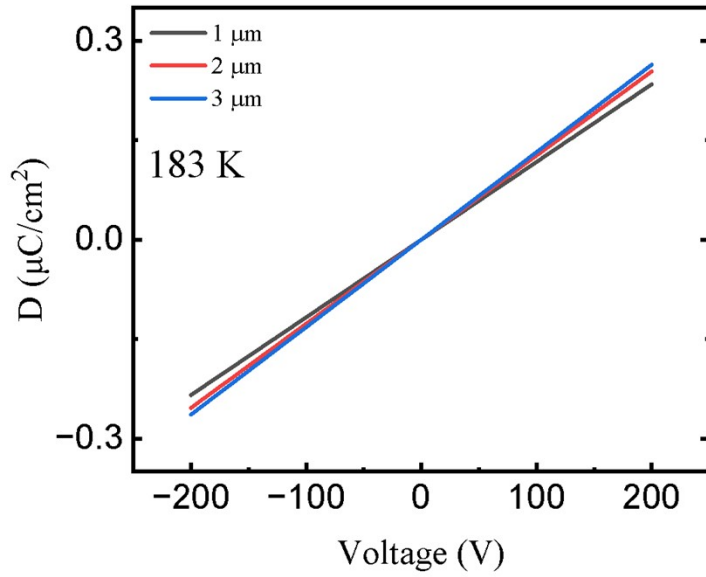


**Figure S5.** D (Electric Displacement) vs V(Voltage) for DC-MBI grown on IDE substrate at 183 K for various thickness.

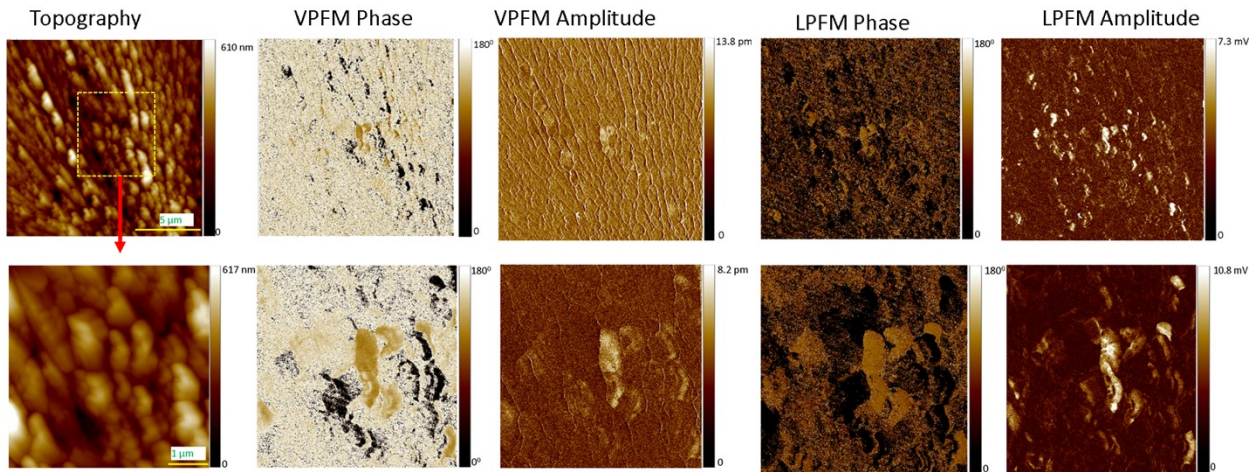


**Figure S6.** PFM measurement performed on the 1  $\mu\text{m}$  thickness sample grown on Au/Si substrate at room temperature. The top row shows the corresponding Topography, VPFM Phase, VPFM Amplitude, LPFM Phase and LPFM Amplitude for 15  $\mu\text{m}$  x 15  $\mu\text{m}$  area while the bottom row is the zoomed over 5  $\mu\text{m}$  x 5  $\mu\text{m}$ . 6V ac bias is used during this scan.

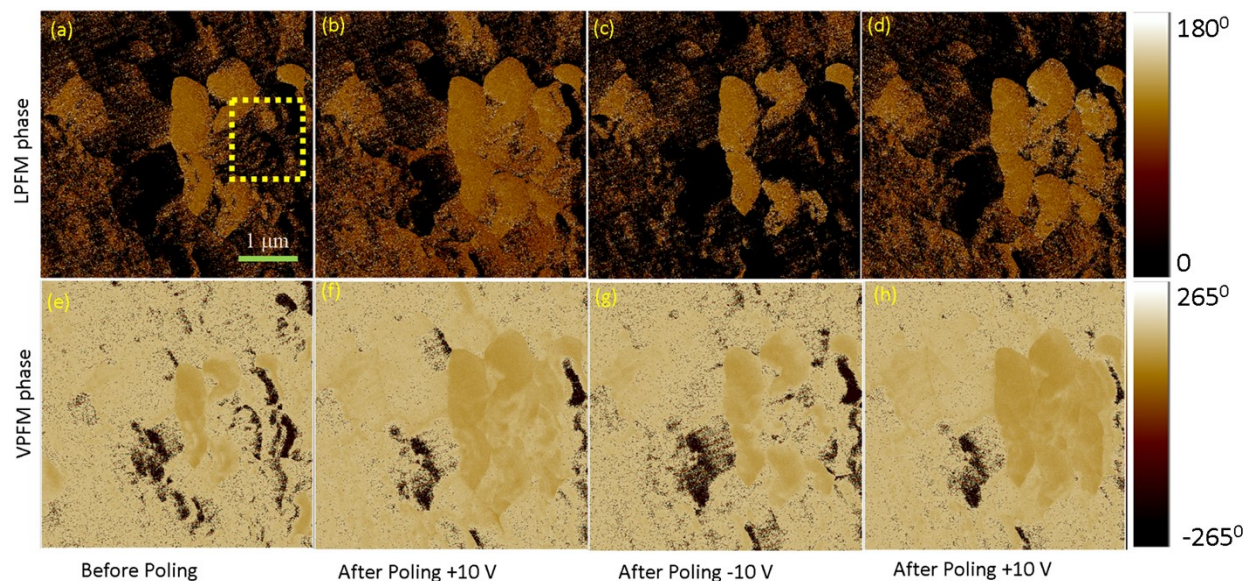


**Figure S7.** PFM Poling experiment with 10 V Tip Bias. The top row represents the LPFM over cycles of poling while the second row is the corresponding VPFM phase.

#### **Supplementary Note 4. Effect of annealing at higher temperature on 2D morphologies**

We find that annealing at higher temperatures rather promotes the 3D growth and even dewetting and evaporation of the films causing the complete destruction of 2D morphologies.



**Figure S8.** Laser microscope images of the 1  $\mu\text{m}$  samples after annealing at 120  $^{\circ}\text{C}$  (30 min) on sapphire substrate (a) over the IDE (b). Fig (c) shows the laser microscope image for the 1  $\mu\text{m}$  sample annealed at 150  $^{\circ}\text{C}$  (15 min) on IDE.

## Supplementary Note 5. FE/DE bilayer model

We can refer to the previously developed FE/DE bilayer model<sup>2</sup> to explain various subtleties of polarizations. We can relate the voids observed on the films (Type-II and Type-III features) can be qualitatively compared to dielectric. **Fig. S9b** shows how the dielectric loading on FE materials can hinder the observable polarizations.

If we use a double FE/DE double layer structure to model the porous structure, the FE loading is then<sup>2</sup>,

$$\frac{\sigma_0}{P_0} = \frac{1}{1 + \varepsilon_F \frac{1-x}{x}} = \frac{1}{1 - \varepsilon_F + \frac{\varepsilon_F}{x}}, \text{ where, } x = \frac{t_F}{t_D + t_F}.$$

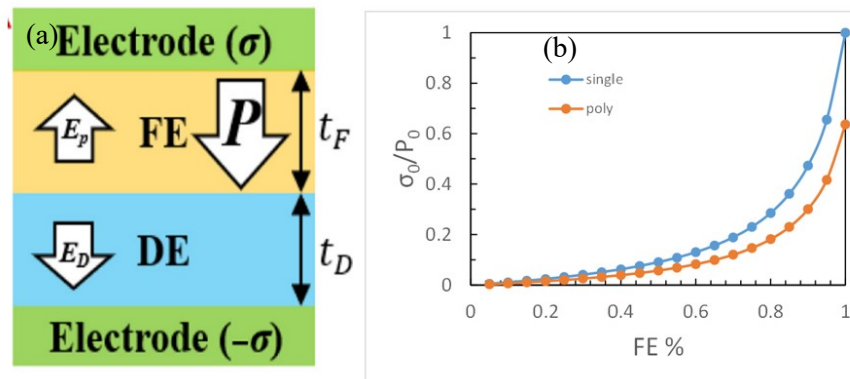


**Figure S9.** FE loading model based on FE/DE double layer structure<sup>1</sup>(a) and measurable polarization vs ferroelectric loading the films (b).

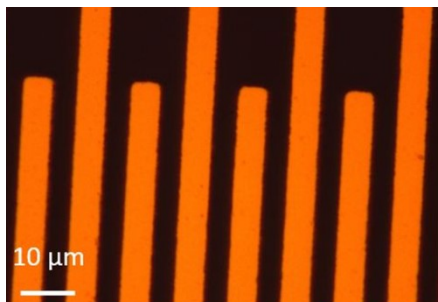


**Figure S10.** Interdigitated electrodes as viewed from optical microscope.

## References

1. Ayiania M, Smith M, Hensley AJR, Scudiero L, McEwen JS, Garcia-Perez M. Deconvoluting the XPS spectra for nitrogen-doped chars: An analysis from first principles. *Carbon N Y.* 2020;162:528-544.  
doi:10.1016/j.carbon.2020.02.065
2. Yun Y, Buragohain P, Thind AS, et al. Spontaneous Polarization in an Ultrathin Improper-Ferroelectric/Dielectric Bilayer in a Capacitor Structure at Cryogenic Temperatures. *Phys Rev Appl.* 2022;18(3):034071.  
doi:10.1103/PHYSREVAPPLIED.18.034071/FIGURES/4/MEDIUM